

# Preparation and Characterization of a Diamagnetic Sulfido-Bridged Divanadium Amide Complex

Mark Moore, Khalil Feghali, and Sandro Gambarotta\*

Department of Chemistry, University of Ottawa, Ottawa, Ontario K1N 6N5, Canada

Received December 16, 1996<sup>⊗</sup>

Reaction of  $[(\text{Me}_3\text{Si})_2\text{N}]_2\text{VCl}(\text{THF})$  with  $\text{S}_8$  led to the formation of the dinuclear and diamagnetic complex  $\{[(\text{Me}_3\text{Si})_2\text{N}]_2\text{V}\}_2(\mu\text{-S})_2$  (**1**), whose connectivity was elucidated by an X-ray crystal structure. *Ab initio* theoretical calculations carried out on both complex **1** and the isostructural oxo-bridged dimer indicated a determinant participation of the bridging atoms in the formation of V–V bonds. Crystal data for **1** are as follows:  $\text{C}_{24}\text{H}_{72}\text{N}_4\text{Si}_8\text{V}_2\text{S}_2$ , fw 807.54, monoclinic  $P2_1/c$ ,  $a = 9.1386(2)$  Å,  $b = 14.5955(3)$  Å,  $c = 34.8578(6)$  Å,  $\beta = 95.744(1)^\circ$ ,  $V = 4626.1(1)$  Å<sup>3</sup>,  $Z = 4$ ,  $T = -153$  °C.

## Introduction

The chemistry of M–M bonds has experienced a steady growth of interest since the original discovery by Brosset of the existence of a short Mo–Mo contact.<sup>1</sup> Today, even though the chemistry of the metal–metal bond is well established and tremendous progress has been achieved toward the understanding of the electronic configurations of the M–M-bonded species,<sup>2</sup> M–M bonds between first-row early transition metals remain less understood. The paradoxical weakness of Cr–Cr supershort quadruple bonds certainly provides a good example in this respect.<sup>3</sup>

The M–M bonding among  $d^1$  first-row metals is even more intriguing since in these systems both the intermetallic distance and the magnetic properties are strongly dependent on the nature of the bridging ligand.<sup>4</sup> Therefore, it is possible that other mechanisms,<sup>5</sup> in addition to direct M–M bonding or antiferromagnetic exchange, may play a crucial role in determining

the efficiency of the electronic coupling between two metal centers. In the particular case of dinuclear vanadium(IV) complexes, there is no straightforward correlation between magnetic behavior and intermetallic separation. Diamagnetic complexes have been obtained with V–V distances up to 2.97 Å,<sup>6</sup> while paramagnetic species have been found with V–V distances as short as 2.514 Å.<sup>7</sup> Even more striking, two divanadium complexes with the same bridging persulfide group have been reported, one being diamagnetic and the other paramagnetic, with long and short intermetallic distances, respectively.<sup>7</sup> This contradictory behavior, together with the broad range of V–V distances as a function of the donor atom,<sup>8</sup> indicates that a V–V bond is unlikely to be significant unless there is a substantial contribution of the bridging atom to its formation.

Recently, Verkade et al. have described the preparation and characterization of the  $\{[(\text{Me}_3\text{Si})_2\text{N}]_2\text{V}\}_2(\mu\text{-O})_2$  dimer featuring a V–V distance of 2.612 Å.<sup>8</sup> The paramagnetism of this species was nicely explained by EHMO calculations with the presence of a pair of nearly degenerate HOMO's primarily metal centered and V–V bonding in character ( $\sigma$  and  $\pi$ ). By using a different synthetic approach, we have now obtained and characterized an essentially isostructural compound,  $\{[(\text{Me}_3\text{Si})_2\text{N}]_2\text{V}\}_2(\mu\text{-S})_2$ , where the bridging oxides were replaced with sulfide. This new compound, *in spite of having a longer intermetallic distance, is diamagnetic*. Herein we describe our findings.

## Experimental Section

All operations were performed under the inert atmosphere of a nitrogen-filled drybox (Vacuum Atmosphere) or by using standard Schlenk techniques. All solvents were freshly distilled from the appropriate drying agent.  $\text{S}_8$  (Aldrich) was used as received.  $[(\text{Me}_3\text{Si})_2\text{N}]_2\text{VCl}(\text{THF})$  was prepared by reacting the corresponding amine with BuLi in hexane and purified by recrystallization in hexane.  $[(\text{Me}_3\text{Si})_2\text{N}]_2\text{VCl}(\text{THF})$  was prepared following published procedures.<sup>9</sup> Infrared spectra

<sup>⊗</sup> Abstract published in *Advance ACS Abstracts*, April 15, 1997.

- (1) Brosset, C. *Ark. Kemi. Miner. Geol.* **1946**, *A20* (7) and *A22* (11).
- (2) (a) Cotton, F. A.; Walton, R. A. *Multiple Bonds Between Metal Atoms*; Wiley: New York, 1982; and references cited therein. (b) Cotton, F. A.; Walton, R. A. *Multiple Bonds Between Metal Atoms*; 2nd ed.; Oxford University Press: Oxford, U.K., 1992; and references cited therein. (c) Troglor, W. C.; Gray, H. B. *Acc. Chem. Res.* **1978**, *11*, 232. (d) Chisholm, M. H.; Foltling, J. C.; Huffman, J. C.; Tatz, R. J. *J. Am. Chem. Soc.* **1984**, *106*, 1153 and references cited therein. (e) Hay, P. J.; Thibeault, J. C.; Hoffman, R. *J. Am. Chem. Soc.* **1975**, *97*, 4884. (f) Poli, R. *Comments Inorg. Chem.* **1992**, *12*, 285. (g) Venturelli, A.; Rauchfuss, T. B. *J. Am. Chem. Soc.* **1994**, *116*, 4824. (h) Cotton, F. A. *Polyhedron* **1987**, *6*, 667. (i) Mingos, D. M. P. *Nature (London)* **1972**, *236*, 99. (j) Losada, J.; Alvarez, J. J. Novoa, F.; Mota, F.; Hoffman, R.; Silvestre, J. *J. Am. Chem. Soc.* **1990**, *112*, 8998. (k) Chisholm, M. H.; Rothwell, I. P. *Prog. Inorg. Chem.* **1982**, *29*, 1. (l) Shaik, S.; Hoffman, R.; Fiesel, C. R.; Summerville, R. H. *J. Am. Chem. Soc.* **1980**, *102*, 4555.
- (3) (a) Benard, M. *J. Am. Chem. Soc.* **1978**, *100*, 2354. (b) Hall, M. B. *Polyhedron* **1987**, *6*, 679. (c) De Mello, P. C.; Edwards, W. D.; Zemer, M. C. *Int. J. Quantum Chem.* **1983**, *23*, 425. (d) Cannon, R. D. *Inorg. Chem.* **1981**, *20*, 241. (e) Wilson, L. M.; Cannon, R. D. *Inorg. Chem.* **1988**, *27*, 2382. (f) Edema, J. J. H.; Gambarotta S. *Comments Inorg. Chem.* **1991**, *11*, 195 and references cited therein. (g) Hao, S.; Edema, J. J. H.; Gambarotta, S.; Bensimon, C. *Inorg. Chem.* **1992**, *31*, 2676. (h) Hao, S.; Gambarotta, S.; Bensimon, C. *J. Am. Chem. Soc.* **1992**, *114*, 3556. (i) Hao, S.; Song, J. I.; Berno, P.; Gambarotta, S. *Organometallics* **1994**, *13*, 1326.
- (4) (a) Wilkinson, G.; Abel, E. W.; Stone, F. G. A. *Comprehensive Organometallic Chemistry*; Pergamon Press: Oxford, U.K., 1982. (b) Wilkinson, G.; Abel, E. W.; Stone, F. G. A. *Comprehensive Organometallic Chemistry II*; Pergamon Press: Oxford, U.K., 1995. (c) Wilkinson, G.; Abel, E. W.; Stone, F. G. A. *Comprehensive Coordination Chemistry*; Pergamon Press: Oxford, U.K., 1987.

- (5) See for example: (a) Hodgson, H. *Proc. Inorg. Chem.* **1975**, *19*, 173. (b) Mabbs, M. B.; Machin, D. J. *Magnetism and Transition Metal Complexes*; Chapman and Hall: London, 1974.
- (6) Preuss, F.; Overhoff, G.; Becker, H.; Hausler, H. J.; Frank, W.; Reiss, G. *Z. Anorg. Allg. Chem.* **1993**, *619*, 1827.
- (7) Bolinger, C. M.; Rauchfuss, T. B.; Rheingold, A. L. *J. Am. Chem. Soc.* **1983**, *105*, 6321.
- (8) Duan, Z.; Schmidt, M.; Young, V. G.; Xie, X.; McCarley, R. E.; Verkade, J. G. *J. Am. Chem. Soc.* **1996**, *118*, 5302 and all references cited therein.
- (9) Berno, P.; Minhas, R.; Hao, S.; Gambarotta, S. *Organometallics* **1994**, *13*, 1052.

were recorded on a Michelson BOMEM FTIR instrument from Nujol mulls prepared in a drybox. Elemental analyses were carried out with a Perkin-Elmer 2000 CHN analyzer. The ratio between V, S, and Si atoms was determined by X-ray fluorescence on a Philips XRF 2400 instrument. Data for X-ray crystal structures were obtained with a Siemens diffractometer equipped with a SMART CCD area detector. Variable-temperature NMR spectra were recorded with a Bruker AMX 500 MHz spectrometer. Theoretical calculations were performed with a Silicon Graphics workstation.

**Preparation of  $\{[(\text{Me}_3\text{Si})_2\text{N}]_2\text{V}\}_2(\mu\text{-S})_2$  (**1**).** A suspension of  $[(\text{Me}_3\text{Si})_2\text{N}]_2\text{VCl}(\text{THF})$  (1.38 g, 2.9 mmol) in toluene (60 mL) was treated at room temperature with  $\text{S}_8$  (0.1 g, 0.39 mmol). The mixture changed rapidly from the original blue green to dark brown red color. After the solution was stirred for about 30 min at room temperature, the solvent was evaporated in vacuo to give a red/brown powder. The residual solid was resuspended in ether (20 mL). The mixture was filtered to eliminate a small amount of insoluble solid. The resulting deep-red solution was allowed to stand at  $-30^\circ\text{C}$  overnight and at  $-78^\circ\text{C}$  for a few days, whereupon crystals of **1** separated (0.25 g, 0.3 mmol, 21%). Anal. Calcd (found) for  $\text{C}_{24}\text{H}_{72}\text{Si}_8\text{N}_4\text{S}_2\text{V}_2$ : C, 35.70 (35.43); H, 8.99 (8.38); N, 6.94 (6.53); S, 7.94 (7.32). IR (Nujol mull, NaCl,  $\text{cm}^{-1}$ ):  $\nu$  1385 (w), 1070 (w), 853 (vs, br), 786 (s), 706 (s), 704 (s), 670 (s), 617 (w).  $^1\text{H-NMR}$  (500 MHz,  $25^\circ\text{C}$ ):  $\delta$  0.51 ( $\text{Me}_3\text{Si}$ ).  $^{13}\text{C-NMR}$  (125.7 MHz,  $25^\circ\text{C}$ ):  $\delta$  8.90.  $^{51}\text{V-NMR}$  (131.4 MHz,  $25^\circ\text{C}$ ):  $\delta$  2531.

**Molecular Orbital Calculations.** All molecular orbital calculations were performed on a Silicon Graphics computer by using the software package SPARTAN 4.0.<sup>10</sup> The program's default parameters were used in the unrestricted and restricted Hartree-Fock *ab initio* calculations on the model  $\{[(\text{H}_3\text{Si})_2\text{N}]_2\text{V}\}_2(\mu\text{-X})_2$  ( $\text{X} = \text{S}, \text{O}$ , respectively) by using the STO-3G basis. The fractional atomic coordinates of the crystal structure were converted to the corresponding cartesian coordinates by using a special device of the NRCVAX program. The methyl group carbon atoms were deleted from the list with the exception of the *ipso* carbons of each ring and replaced by hydrogen atoms introduced at their idealized positions. The resulting symmetry of the molecule was  $C_1$  thus reflecting the crystallographic symmetry of complex **1**. Calculations were also performed by imposing higher symmetries, without significantly modifying the final results. The results of the calculations presented in this work were obtained by using a  $C_{2v}$  symmetry.

**X-ray Crystallography.** Data were collected at  $-153^\circ\text{C}$  using the  $\omega$ - $2\theta$  scan technique to a maximum  $2\theta$  value of  $45.0^\circ$  for a suitable crystal mounted on glass fibers. Cell constants and orientation matrices were obtained from the least-squares refinement of 25 carefully centered high-angle reflections. Redundant reflections were averaged. The intensities of three representative reflections were measured after every 150 reflections to monitor crystal and instrument stability. Data were corrected for Lorentz and polarization effects but not for absorption. The structures were solved by direct methods. The positions of the non-hydrogen atoms were refined anisotropically. A few of the methyl group carbon atoms display rather large thermal parameters possibly indicative of thermal disorder. Attempts to model this minor disorder by splitting the occupancy over several positions failed. Hydrogen atom positions were introduced at their idealized positions. The final cycle of full-matrix least-squares refinement was based on the number of observed reflections with  $I > 2.5\sigma(I)$ . Neutral atomic scattering factors were taken from Cromer and Waber.<sup>11</sup> Anomalous dispersion effects were included in  $F_c$ . All calculations were performed using a NRCVAX package on a Silicon Graphics workstation. Details on crystal data and structure solution are given in Table 1. Selected bond distances and bond angles are given in Table 2. Listing of atomic coordinates and thermal parameters are given as Supporting Information.

## Results and Discussion

The reaction of  $[(\text{Me}_3\text{Si})_2\text{N}]_2\text{VCl}(\text{THF})$  with  $\text{S}_8$  proceeded rapidly in toluene at room temperature to provide a dark red/

**Table 1.** Crystal Data and Structure Analysis Results for **1**

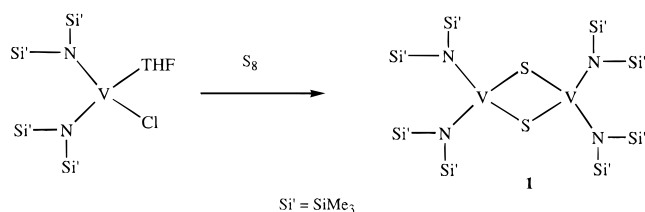
empirical formula	$\text{C}_{24}\text{H}_{72}\text{N}_4\text{Si}_8\text{V}_2\text{S}_2$
fw	807.54
space group	monoclinic, $P2_1/c$
$a$ (Å)	9.1386(2)
$b$ (Å)	14.5955(3)
$c$ (Å)	34.8578(6)
$\beta$ (deg)	95.744(1)
$V$ (Å <sup>3</sup> )	4626.1(1)
$Z$	4
radiation (Å)	Mo K $\alpha$ ( $\lambda = 0.70930$ )
$T$ (°C)	-153
$D_{\text{calcd}}$ ( $\text{g cm}^{-3}$ )	1.159
$\mu_{\text{calcd}}$ ( $\text{cm}^{-1}$ )	7.0
$R_w^a$ $R_w^a$	0.050, 0.047

$$^a R = \sum ||F_o| - |F_c|| / \sum |F_o|. R_w = [(\sum (|F_o| - |F_c|)^2 / \sum w F_o^2)]^{1/2}.$$

**Table 2.** Selected Bond Distances (Å) and Angles (deg) for **1**

V1-V2	2.857(1)	V1-S1	2.211(1)
V1-S2	2.206(1)	V2-S1	2.216(1)
V2-S2	2.206(2)	V1-N1	1.878(4)
V1-N2	1.874(4)	V2-N3	1.857(4)
V2-N4	1.882(4)	N1-Si1	1.773(4)
N1-Si2	1.784(4)	S1-S2	3.336(1)
S1-V1-S2	98.12(6)	V1-S2-V2	82.04(5)
S2-V2-S1	97.94(6)	V1-S1-V2	81.70(5)
N3-V2-S1	110.7(1)	N3-V2-S2	107.8(1)
N3-V2-N4	115.3(2)	N4-V2-S1	109.1(1)
N4-V2-S2	114.6(1)	V1-N2-Si3	115.3(2)
V1-N2-Si4	128.7(2)	Si3-N2-Si4	115.8(2)

## Scheme 1



brown mixture (Scheme 1). After suitable workup, moderately air-stable, dark brown-red crystals of a complex formulated as  $\{[(\text{Me}_3\text{Si})_2\text{N}]_2\text{V}\}_2(\mu\text{-S})_2$  (**1**) were obtained in moderate yield. The formulation was supported by combustion analysis data. The only notable feature of the IR spectrum was an intense and broad band of the trimethylsilyl group centered at  $853\text{ cm}^{-1}$ . Qualitative tests showed the presence of sulfur and the absence of chlorine.

Complex **1** is diamagnetic in both the solid state and solution. Multinuclear NMR spectroscopy yielded well-resolved spectra with the resonances in the expected positions. Only the resonance of  $^{51}\text{V}$  (+2531 ppm) was considerably shifted,<sup>12</sup> possibly indicating the presence of a minor residual paramagnetism. However, variable-temperature NMR experiments did not show any significant variation of the chemical shift as a function of the temperature.

The formation of **1** occurs through a complicated reaction that requires ligand scrambling in addition to the oxidation of the metal center. During the formation of the complex the chlorine atom probably migrates to form another reaction coproduct. Even though we do have evidence for the formation of another species, efforts to clarify the nature and the structure of this second product have thus far failed.

The structure and the molecular connectivity were elucidated by single-crystal X-ray analysis. The structure is formed by two

(10) All the calculations were performed with the software package SPARTAN 4.0, Wavefunction, Inc., 18401 Von Karman Av., #370, Irvine, CA 92715, 1995.

(11) Cromer, D. T.; Waber, J. T. *International Tables for X-ray Crystallography*; The Kynoch Press: Birmingham, England, 1974.

(12) The usual range of  $^{51}\text{V-NMR}$  chemical shift is  $\pm 2000$  ppm. (a) Rehder, D. *Coord. Chem. Rev.* **1991**, *110*, 161. (b) Rehder, D. In *Advanced Applications of NMR to Organometallic Chemistry*; Wrackmeyer, B., Gielen, M., Willem, R., Eds.; Wiley: New York, in press.

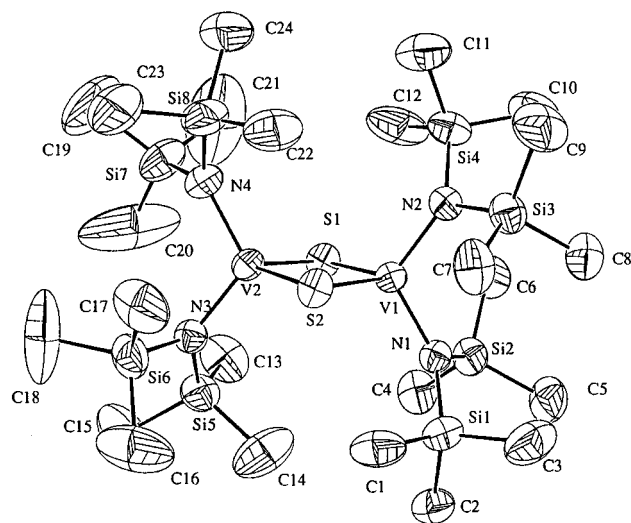


**Figure 1.** ORTEP plot of **1**. Thermal ellipsoids are drawn at the 50% probability level.

almost identical  $\{(\text{Me}_3\text{Si})_2\text{N}\}_2\text{V}$  units bridged by two sulfur atoms. The coordination geometry around each vanadium atom is distorted tetrahedral [ $\text{N1-V1-S1} = 108.8(1)^\circ$ ,  $\text{N1-V1-S2} = 111.7(1)^\circ$ ,  $\text{N1-V1-N2} = 114.8(2)^\circ$ ,  $\text{N2-V1-S1} = 111.2(1)^\circ$ ,  $\text{N2-V1-S2} = 108.0(1)^\circ$ ] and is defined by two nitrogens [ $\text{V1-N1} = 1.878(4) \text{ \AA}$ ,  $\text{V1-N2} = 1.874(4) \text{ \AA}$ ] of the two amide groups and the two bridging sulfur atoms. The distortion around vanadium is probably caused by the steric bulk of the two large trimethylsilyl groups [ $\text{N1-V1-N2} = 114.8(1)^\circ$ ,  $\text{N3-V2-N4} = 115.3(2)^\circ$ ]. The coordination geometry around each nitrogen atom is trigonal planar [ $\text{V1-N1-Si1} = 130.4(2)^\circ$ ,  $\text{V1-N1-Si2} = 113.8(2)^\circ$ ,  $\text{S1-N1-Si2} = 115.7(2)^\circ$ ] with rather short V-N distances. The  $\text{V}_2\text{S}_2$  core is nearly planar [ $\text{S1-V1-S2-V2} = 3.4(1)^\circ$  torsion angle] with rather short V-S distances [ $\text{V1-S1} = 2.211(1) \text{ \AA}$ ,  $\text{V1-S2} = 2.206(1) \text{ \AA}$ ,  $\text{V2-S1} = 2.216(1) \text{ \AA}$ ,  $\text{V2-S2} = 2.206(2) \text{ \AA}$ ] possibly indicative of some V-S multiple bond character. The angles subtended at the bridging sulfur atoms are rather small [ $\text{V1-S1-V2} = 81.70(5)^\circ$ ,  $\text{V1-S2-V2} = 82.04(5)^\circ$ ] but compare well with other similar  $\text{M}_2\text{S}_2$  frameworks.<sup>13,14</sup>

The long V-V distance [ $\text{V1}\cdots\text{V2} = 2.857(1) \text{ \AA}$ ] and the diamagnetism of **1** raises questions about the nature of the intermetallic interaction and the possible mechanism for the magnetic coupling between the two  $d^1$  metal centers. A database search on dinuclear tetravalent vanadium complexes yielded 31 crystal structures.<sup>8</sup> In all of these  $d^1$  species the  $\text{M}_2\text{X}_2$  cores featured intermetallic separations ranging from 2.459 to 3.033  $\text{ \AA}$  depending on the nature of the bridging ligands. In the case of complex **1**, the longer intermetallic distance with respect to  $\{[(\text{Me}_3\text{Si})_2\text{N}]_2\text{V}\}_2(\mu\text{-O})_2$  (0.25  $\text{ \AA}$ ) is not surprising given the larger atomic dimensions of the bridging atom (S versus O) and the consequent longer V-S distances with respect to V-O. However, the fact that in the identical ligand system the elongation of the intermetallic distance led to a more efficient coupling of the  $d^1$  electrons seems to indicate that a significant V-V bond is unlikely to exist in complex **1**. The angles subtended at the bridging sulfur atoms, significantly narrower

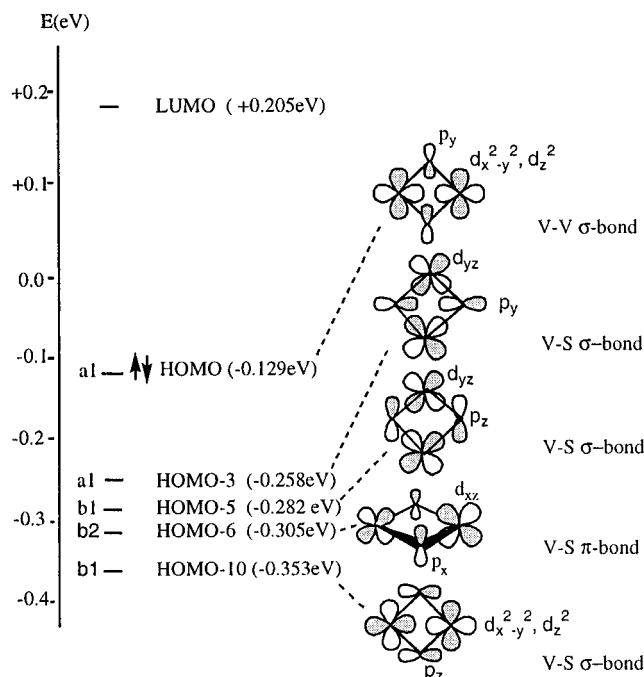


**Figure 2.** Schematic representation of the energy level diagram for  $\{[(\text{H}_3\text{Si})_2\text{N}]_2\text{V}\}_2(\mu\text{-S})_2$  showing the most relevant molecular orbitals.

than  $90^\circ$ , are possibly the result of the tetrahedral coordination geometry of vanadium which dictates relatively large S-V-S angles. In addition, angles as narrow as  $71^\circ$  are rather common among sulfide- and persulfide-bridged divanadium complexes,<sup>14a,d</sup> which are almost invariably diamagnetic regardless of the size of intermetallic separation (typically in the range 2.5–2.87  $\text{ \AA}$ ).<sup>7,14</sup> The conclusion emerging from these observations is that the nature of the donor atom and geometry optimization are indeed crucial for the efficiency of the magnetic coupling between the two metal centers. Thus in an attempt to clarify the nature of the V-V interaction in these two complexes we have carried out *ab initio* unrestricted HF/STO-36 calculations using  $\{[(\text{H}_3\text{Si})_2\text{N}]_2\text{V}\}_2(\mu\text{-S})_2$  as a model.<sup>15</sup> The geometrical parameters of the non-hydrogen atoms were those obtained from the X-ray crystal structure. The HOMO-LUMO gap is not particularly large (0.334 eV), but it is still sufficient to account for the diamagnetism. Of the 121 populated bonding MOs only the HOMO ( $-0.129 \text{ eV}$ ) showed a significant V-V bond character. This molecular orbital (Figure 2) is mainly generated by the overlap of two identical hybrid combinations of  $d_{x^2-y^2}$  and  $d_{z^2}$  atomic orbitals (MO factor 0.44 and 0.43, respectively) of each vanadium atom with the  $p_y$  orbitals of the bridging sulfur atoms. The shape of this orbital, which lies on the intermetallic vector, is strongly reminiscent of a M-M  $\sigma$ -bond. However, the overlap between the vanadium orbitals seems to be rather weak, and the contribution of the sulfur  $p_y$  orbitals to its formation (MO factor = 0.13) is significant. The next two lower MOs are located at  $-0.224$  and  $-0.231 \text{ eV}$  and are mainly sulfur-centered with a minor V-S  $\pi$  character. Two V-S  $\sigma$ -bonds, mainly arising from the overlap of the vanadium  $d_{yz}$  orbitals with the  $p$  orbitals of the two sulfur atoms, are respectively the HOMO-3 ( $-0.258 \text{ eV}$ ) and HOMO-5 ( $-0.282 \text{ eV}$ ). A third V-S  $\sigma$ -bond (HOMO-10) was located lower in energy at  $-0.353 \text{ eV}$ . This orbital is constructed from the same combination of vanadium atomic orbitals which form the V-V  $\sigma$ -bond and the  $p_z$  orbitals of the bridging sulfur atoms. A V-S

(13)  $\text{Ti}_2\text{S}_2$ : Scoles, L.; Gambarotta, S. *Inorg. Chim. Acta* **1995**, 235, 375.  $\text{Cr}_2\text{S}_2$ : Reardon, D.; Kovacs, I.; Gambarotta, S.; Thompson, L.; Petersen, J., manuscript in preparation.

(14) (a) Bolinger, C. M.; Rauchfuss, T. B.; Rheingold, A. L. *Organometallics* **1982**, 1, 1551. (b) Helbert, T. R.; Hutchings, L. L.; Rhodes, R.; Stiefel, E. I. *J. Am. Chem. Soc.* **1986**, 108, 6437. (c) Sendlinger, S. C.; Nicholson, J. R.; Lobkovsky, E. B.; Huffman, J. C.; Rehder, D.; Christou, G. *Inorg. Chem.* **1993**, 32, 204. (d) Duraj, S. A.; Andras, M. T.; Kibala, P. A. *Inorg. Chem.* **1990**, 29, 1232.

(15) The intermetallic vector was selected as the  $z$  axis and the X-X vector (X = S, O) as the  $y$  axis, while the  $x$  axis was perpendicular to the plane of the  $\text{V}_2\text{X}_2$  core.

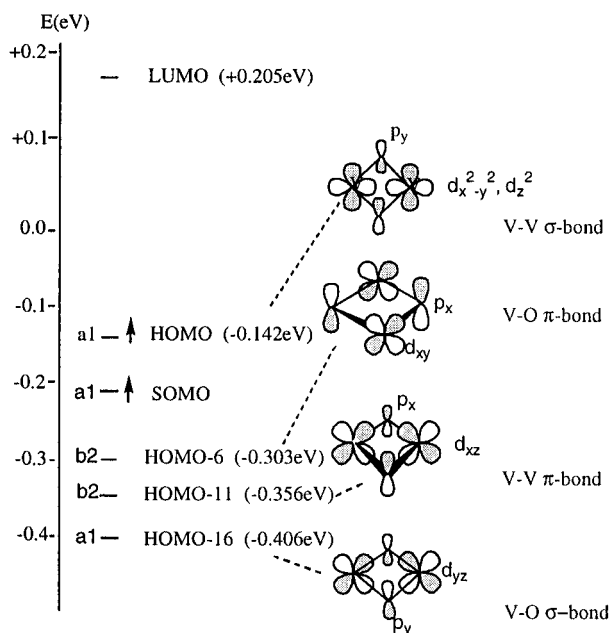


**Figure 3.** Schematic representation of the energy level diagram for  $\{[(\text{H}_3\text{Si})_2\text{N}]_2\text{V}_2(\mu\text{-O})_2\}$  showing the most relevant molecular orbitals.

$\pi$ -bond (HOMO-6) was found at  $-0.305$  eV and is formed by the combination of the vanadium  $d_{xz}$  orbitals with the  $p_x$  orbitals of the two sulfur atoms forming two largely delocalized lobes on the two sides of the  $\text{V}_2\text{S}_2$  plane, thus conferring a formal bond order significantly higher than unity to the V–S bond (average V–S bond order = 1.22). This bond has a weak V–V  $\pi$ -bond character. The amido nitrogen atoms p orbitals also significantly contribute to the formation of this largely delocalized molecular orbital.

The results of these calculations clearly indicate that the magnetic coupling between the two metal centers of **1** is mainly realized via a direct V–V  $\sigma$ -bond. While this is not particularly surprising *per se*, it makes the paramagnetism of the corresponding oxo analogue even more difficult to understand especially when considering that this species has a considerably shorter V–V distance. In fact one could reasonably expect that if the magnetic coupling in complex **1** is realized via a direct V–V interaction, the shorter intermetallic distance of the oxo analogue should lead to an even better overlap of the d orbitals. Since this is in contrast to the experimental observations, we have recalculated the oxo derivative by using the same *ab initio* theoretical approach.<sup>15</sup> The energy gap between the LUMO and the singly occupied HOMO (0.347 eV) compares well with that calculated for compound **1**. The HOMO and the SOMO are located respectively at  $-0.142$  and  $-0.205$  eV and are very different in character. Similar to complex **1**, the HOMO is mainly a V–V centered molecular orbital and is formed by the same hybrid combination of  $d_{x^2-y^2}$  and  $d_z^2$  (MO factors = 0.42 and 0.43, respectively) atomic orbitals of the vanadium atoms with the  $p_y$  orbitals of the two oxygen atoms (Figure 3). The difference with respect to the analogous orbital of complex **1** is that the contribution of the  $p_y$  orbital of the bridging atoms is now more pronounced (MO factor = 0.21) than in the case of sulfur, probably as a result of the shorter V–V distance. The

next singly populated MO orbital (SOMO  $-0.205$  eV) is nonbonding with respect to V–V. A  $\pi$  molecular orbital (HOMO-11,  $-0.356$  eV), mainly originating from the overlap of the  $d_{xz}$  of the two vanadium atoms and the  $p_x$  orbitals of the two oxygens, forms two large lobes delocalized on the two sides of the  $\text{V}_2\text{O}_2$  plane. Although this orbital has some V–V  $\pi$ -bond character, the contribution of the oxygen atomic orbitals is comparable (MO coefficient 0.22) to that of the vanadium d orbitals (MO coefficient 0.31). The combination of atomic orbitals which composes this particular MO is the same as that which composes the V–S  $\pi$ -orbitals of complex **1**. However, while in the case of **1** the V–V  $\pi$ -bond character is only minor, it appears to be more significant in the oxide case. Once again this is probably the result of the shorter intermetallic distance caused by the two bridging oxides. The formation of two different V–V bonds, both  $\sigma$  and  $\pi$  in character, is in good qualitative agreement with the results of the previously reported EHMO calculation.<sup>8</sup> A V–O–V  $\pi$ -bond is found at  $-0.303$  eV (HOMO-6) and is mainly generated by the  $\pi$ -overlap of the  $d_{xy}$  of the two vanadium atoms and the  $p_x$  orbitals of the two bridging oxides. Curiously such an orbital was not found in the case of complex **1**. The V–O–V  $\sigma$ -bond was located at  $-0.406$  eV (HOMO-16) and is formed by the overlap of the vanadium  $d_{yz}$  orbitals with the  $p_y$  of the oxygens.

On the basis of this theoretical work, we are unable to provide a simple and straightforward explanation of the striking difference between the magnetic properties of the two complexes other than trivial arguments based on the near HOMO–SOMO degeneracy. We observed that, in the case of **1**, at least two MOs (HOMO-9 and -16) show a significant S–S  $\sigma$ -bond character. Similar orbitals are not present among the MOs of the oxo-bridged complex. On the other hand, given the long S–S distance (3.3 Å), we are unable to evaluate the significance of these orbitals and the relative contribution of this additional interaction to the coupling of the d electrons. However, these MOs involve a rather substantial participation of the vanadium orbitals. At this stage it is tempting to speculate that this additional S–S interaction plays an important role in determining the diamagnetism of complex **1**.

The di- $\mu$ -X-bridged species examined in this work at best have 2-fold rotation symmetry and thus must have only nondegenerate MO's based upon symmetry alone. The bonding interactions then dictate whether the HOMO–LUMO gap will be large enough to give spin-pairing (assuming even-electron systems) or small enough to give singly-occupied levels with triplet or higher spin states. Clearly both the direct M–M interactions and the M–X and/or M–L interactions will be important in determining the gap energy. MO calculations are needed in the individual cases in order to make these assessments.

**Acknowledgment.** This work was supported by the Natural Sciences and Engineering Research Council of Canada (NSERC) through strategic and operating grants.

**Supporting Information Available:** Tables of crystal data, atomic coordinates, thermal parameters, and bond distances and angles for **1** (11 pages). Ordering information is given on any current masthead page.

IC961471I